

# Distributed Acoustic Sensing With Michelson Interferometer Demodulation

Xiaohui LIU<sup>1</sup>, Chen WANG<sup>1</sup>, Ying SHANG<sup>1</sup>, Chang WANG<sup>1\*</sup>, Wenan ZHAO<sup>1</sup>,  
Gangding PENG<sup>1,2</sup>, and Hongzhong WANG<sup>3</sup>

<sup>1</sup>Shandong Key Laboratory of Optical Fiber Sensing Technologies, Laser Institute of Shandong Academy of Sciences, Jinan, Shandong, 250014, China

<sup>2</sup>School of Electrical Engineering & Telecommunications, the University of New South Wales, NSW, 2052, Australia

<sup>3</sup>Shengli Oilfield Xinsheng Geophysical Technology Co. Ltd., Dongying, Shandong, 257000, China

\*Corresponding author: Chang WANG E-mail: wang960100@163.com

**Abstract:** The distributed acoustic sensing (DAS) has been extensively studied and widely used. A distributed acoustic sensing system based on the unbalanced Michelson interferometer with phase generated carrier (PGC) demodulation was designed and tested. The system could directly obtain the phase, amplitude, frequency response, and location information of sound wave at the same time and measurement at all points along the sensing fiber simultaneously. Experiments showed that the system successfully measured the acoustic signals with a phase-pressure sensitivity about  $-148$  dB (re rad/ $\mu$ Pa) and frequency response ripple less than 1.5 dB. The further field experiment showed that the system could measure signals at all points along the sensing fiber simultaneously.

**Keywords:** Distributed acoustic sensing; phase generated carrier; interferometer; frequency response

---

Citation: Xiaohui LIU, Chen WANG, Ying SHANG, Chang WANG, Wenan ZHAO, Gangding PENG, *et al.*, "Distributed Acoustic Sensing With Michelson Interferometer Demodulation," *Photonic Sensors*, 2017, 7(3): 193–198.

---

## 1. Introduction

Distributed acoustic sensing (DAS) is a novel technology which offers the capability of measurement at thousands of points simultaneously, using a simple and unmodified optical fiber as the sensing element. Compared with conventional point sensors, DAS needs no special reflectors or fiber Bragg gratings in its optical path, which greatly reduces the operation difficulty in field test. And it can measure thousands of continuous points along the sensing fiber and form acoustic or seismic imaging. These advantages cause DAS to be extensively studied and widely used in the fields of

oil and gas exploration, national defense, security, and so on [1–5].

The DAS system operates according to a radar-style process: it sends a series of pulses into the fiber and records the return of the naturally occurring scattered signal against time. One representative of this backscattered sensing is phase sensitive optical time domain reflectometer ( $\varphi$ -OTDR), which inputs a narrow line-width laser to the sensing fiber and monitors the phase changes of Rayleigh backscattered lights [6–9]. The other one is Brillouin optical time domain reflectometer (BOTDR) which uses Brillouin backscattered lights to measure dynamic strain and temperature [10–12].

---

Received: 7 July 2016 / Revised: 9 November 2016

© The Author(s) 2017. This article is published with open access at Springerlink.com

DOI: 10.1007/s13320-017-0363-y

Article type: Regular

A major limitation of these distributed sensors above is that they are incapable of determining the full vector acoustic field, namely the amplitude, frequency, and phase, which is a necessity for acoustic or seismic imaging. Measuring the full acoustic field is a much harder technical challenge to be overcome. But, in doing this, it is possible to achieve high resolution seismic imaging and also make other novel systems, for example, a massive acoustic antenna.

In this work, a DAS system based on the Michelson interferometer with phase generated carrier (PGC) demodulation was designed and tested. Experiments showed that the system could successfully acquire the acoustic signal information, including the location, frequency, amplitude, and phase, at all points along the sensing fiber simultaneously.

## 2. System design

The DAS system diagram is shown in Fig. 1. The light source used in the system is a distributed-feedback laser diode (DFB-LD) which emits a continuous wave light with the power of 10 mW and linewidth of 5 kHz. The light is injected into an acoustic-optic modulator (AOM) to generate a pulsed light. The pulses of the light have the width of 50 ns and repetition rate  $R$  of 50 kHz. Then the modulated pulses are amplified by an erbium-doped fiber amplifier (EDFA) in which a narrow-band light filter is integrated to remove the spontaneous

emission noise. Then the amplified pulses are launched into a single mode sensing fiber (Corning SMF-28e) by a circulator, and the Rayleigh-backscattered light is excited at all positions of the sensing fiber. When an acoustic signal is applied on a position of the sensing fiber, it changes the optical path difference of the two backscattered lights exited ahead and behind of the position. So we can introduce an unbalanced interferometer to make the two neighborhood-position's Rayleigh-backscattered lights interfere and obtain the acoustic signal. The backscattered light is amplified by another EDFA to improve the signal-to-noise-ratio (SNR). Then the amplified light passes through an isolator and is injected into a Michelson interferometer which consists of a  $2 \times 2$  coupler, a phase modulator (PM), and two Faraday rotation mirrors (FRMs). The light is split into two equal beams by the coupler. One of the beams is modulated by the PM with the 2-kHz sinusoidal wave to generate the phase carrier, which decides that the highest signal frequency measured is no more than 1 kHz theoretically. The length difference of two interferometer arms is 5 m. The final interference signals outputted from the coupler are detected by a photodetector (PD) and digitized by an analog to digital (A/D) converter. Then the digitized signals are arrayed according to the position of the sensing fiber. Then the signals processing scheme is accomplished by a software program of PGC demodulation.

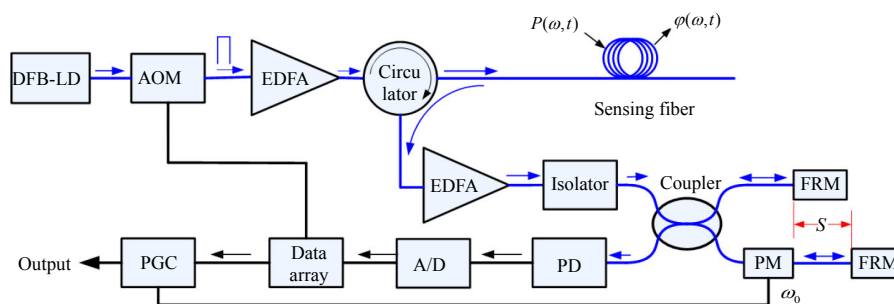


Fig. 1 DAS system block diagram.

The interferometer output signal  $I$  can be expressed as

$$I = A + B \cos[C \cos \omega_0 t + \psi(t)] \quad (1)$$

where  $A$  is the average optical power of the interferometer output signal.  $B = kA$ ,  $k \leq 1$ , and  $k$  is the interference fringe visibility.  $C \cos \omega_0 t$  is the phase generated carrier.  $\psi(t) = \varphi(\omega, t) + \phi(t)$ ,  $\varphi(\omega, t)$  is the phase change induced by the acoustic signal, and  $\phi(t)$  is the slow variation of the initial phase caused by the environment.

The PGC demodulation scheme is shown in

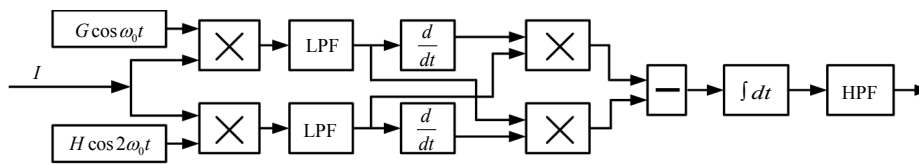


Fig. 2 PGC demodulation scheme.

By introducing the unbalanced interferometer with a arm-length difference of 5 m, the signal we got every time represents the phase change between two points of 5 m apart on the sensing fiber. That is to say, the spatial resolution of the system is 5 m. The repetition rate of the pulses decides the system's maximum detection length. The time interval between two pulses should be longer than the round trip time of the light traveling in the sensing fiber to insure that there is only one pulse inside the fiber at any time. For the 50-kHz repetition rate, we can know that the detection range is around 2 km which is determined by  $L < c/2Rn_f$ .

### 3. Lab experiments

A water tank system was used to examine the performance of the DAS system (Fig. 3). An underwater speaker was fixed in water and driven by a function generator. A sensing fiber with a length of 10 m was wrapped into a fiber ring with a diameter of 8 cm to reduce the influence of the acoustic-intensity differences, which was put into water and connected to the DAS instrument. A commercial piezoelectric hydrophone (Type

Fig. 2. The interferometer output signal  $I$  is fed into the PGC demodulation scheme, and the final output of the system, which contains the tested signal  $\varphi(\omega, t)$ , is [13]

$$B^2 G H J_1(C) J_2(C) \phi(\omega, t) \equiv K \phi(\omega, t) \quad (2)$$

where  $G$  and  $H$  are the amplitude of fundamental and double frequency signal, respectively.  $K = B^2 G H J_1(C) J_2(C)$  is the gain factor of the system. Finally, we calibrate the constant  $K$  and obtain the acoustic signal from the high-pass filter (HPF).

RHSA20 made by 715th Research Institute of China Shipbuilding Industry Corporation) was also placed close to the fiber ring to measure the acoustic pressure amplitude. The sound fields of the fiber ring and the piezoelectric hydrophone were almost the same.

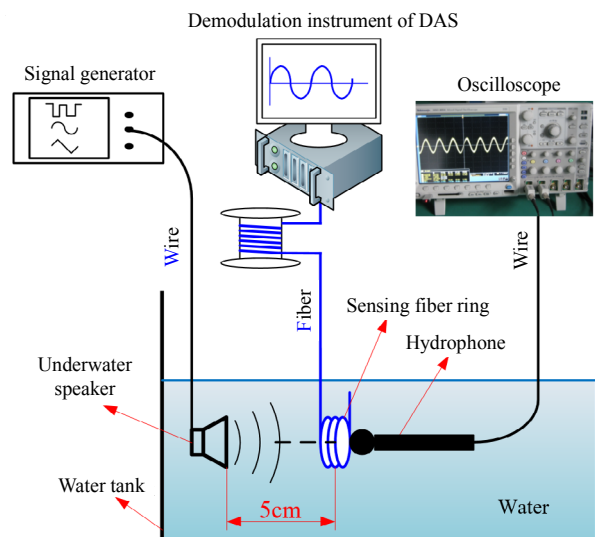


Fig. 3 Schematic diagram of underwater experiment.

Firstly, we fixed the frequency at 200 Hz and changed the amplitude of the sinusoidal wave generated by the function generator. The acoustic

pressure amplitudes in different acoustic intensities were measured by the piezoelectric hydrophone, and the phase-pressure sensitivity of the DAS system was calculated. Figure 4 shows the instantaneous frequency of our system demodulated and the spectral analysis via fast Fourier transform (FFT) of the demodulated signal. It indicates that the signals of DAS and hydrophone have almost the same waveform and SNR. It demonstrates that the DAS system can measure the full vector acoustic field,

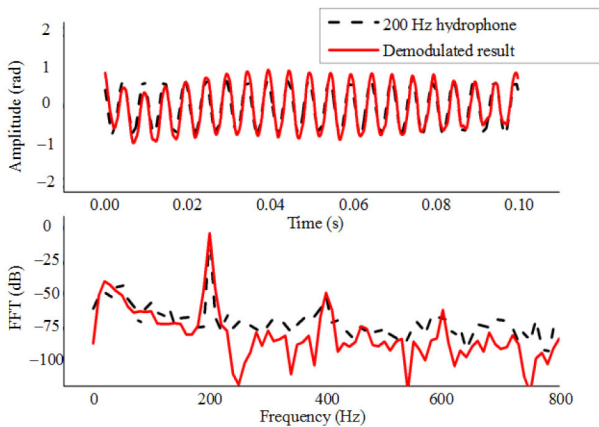


Fig. 4 Signals of DAS sensor and hydrophone.

Secondly, we fixed the amplitude and changed the frequency of the sinusoidal wave generated by the function generator to measure the frequency response of our system. Figure 6 shows the frequency response of the system from 50 Hz to 500 Hz. The response flatness of less than 1.5 dB was obtained.

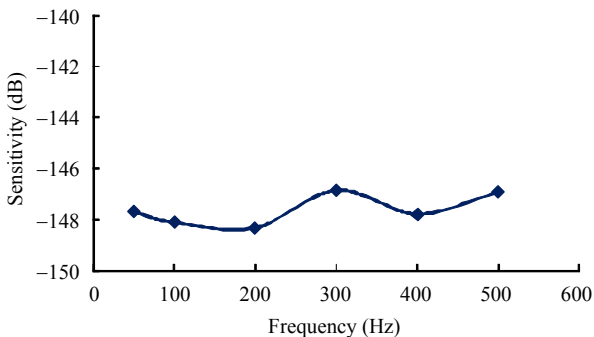


Fig. 6 DAS frequency response curve.

including the amplitude, frequency, and phase. Figure 5 shows the phase-pressure relationship of the DAS system. When the acoustic pressure increases, the demodulated phase variation increases linearly. The phase-pressure sensitivity was calculated through our system demodulated phase amplitude divided by piezoelectric hydrophone detected acoustic pressure amplitude. The achieved phase-pressure sensitivity was 0.0384 rad/Pa ( $-148$  dB, re rad/ $\mu$ Pa).

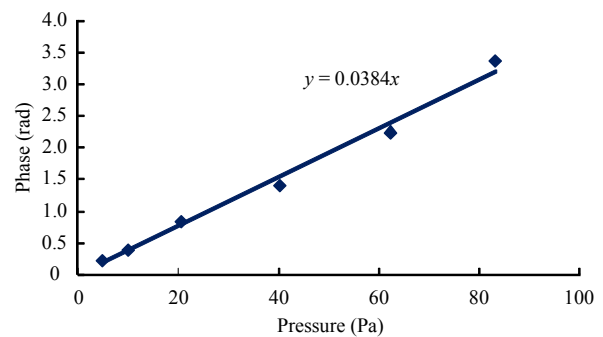


Fig. 5 Phase-pressure relationship.

#### 4. Field experiments

Furthermore, a field experiment was introduced to examine the system. We buried a 110-m-long fiber cable with 50 cm underneath the ground, which was marked from 33 m to 143 m shown in Fig. 7. And a man walked on the ground along the buried fiber cable. The fiber cable was connected to the DAS instrument in which there was a monitor program running to process the acoustic signals of all the points on the fiber cable in real time. The output of the program is shown in Fig. 8. The gray level represents the intensity, which is the square of the amplitude of the acoustic signal we tested. According to the figure, we can clearly identify the signal of every walking step and infer the man walking 19 steps in 10 s and about 15 m forward. So the signals at all points along the sensing fiber can be measured by the DAS system simultaneously.

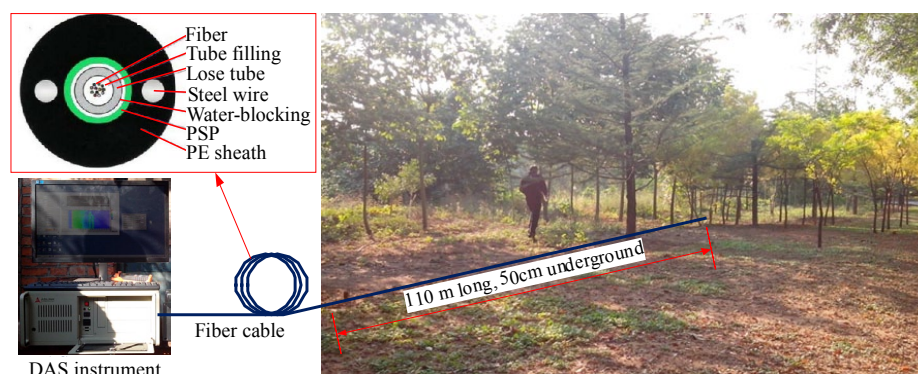


Fig. 7 Schematic diagram of walking experiment.

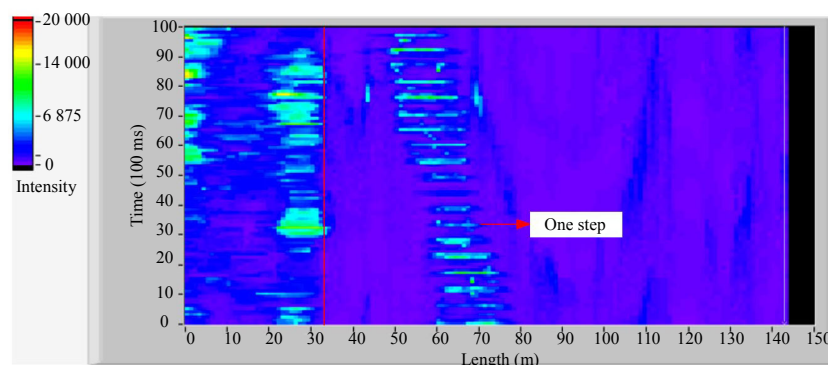


Fig. 8 Output of DAS instrument program.

## 5. Conclusions

An optical fiber distributed acoustic sensing system based on the unbalanced Michelson interferometer and PGC demodulation is demonstrated. The system can directly obtain the phase, amplitude, frequency response, and location information of sound wave at the same time and measure at all points along the sensing fiber simultaneously. Experiments showed that the system successfully measured the acoustic signals with the phase-pressure sensitivity of about  $-148$  dB (re rad/ $\mu$ Pa) and frequency response flatness of less than 1.5 dB. The further field experiment showed that the system could measure signals at all points along the sensing fiber simultaneously. The DAS can be used as geophone for surface, seabed, and downhole measurements, encompassing vertical seismic profiles. It can also offer integrity and surveillance monitoring solutions for pipelines and intrusions by using a single optical fiber cable.

## Acknowledgment

This work was supported by Science and Technology Development Projects (Nos. 2014GGX103019 and 2015GSF120001) of Shandong Province, and Independent Innovation Major Project (No. 2014ZZCX04206) of Shandong Province.

**Open Access** This article is distributed under the terms of the Creative Commons Attribution 4.0 International License (<http://creativecommons.org/licenses/by/4.0/>), which permits unrestricted use, distribution, and reproduction in any medium, provided you give appropriate credit to the original author(s) and the source, provide a link to the Creative Commons license, and indicate if changes were made.

## References

- [1] M. D. Thomas, M. F. Barry, A. Jonathan, and S. Dou, "Field testing of fiber-optic distributed acoustic sensing (DAS) for subsurface seismic monitoring," *Leading Edge*, 2013, 32(6): 699–706.

- [2] A. Mateeva, J. Lopez, H. Potters, J. Mestayer, B. Cox, D. Kiyashchenko, *et al.*, "Distributed acoustic sensing for reservoir monitoring with vertical seismic profiling," *Geophysical Prospecting*, 2014, 62(4): 679–692.
- [3] M. Mondanos, T. Parkera, C. H. Milnea, J. Yeoa, T. Colemana, and M. Farhadiroushana, "Distributed temperature and distributed acoustic sensing for remote and harsh environments," *SPIE*, 2015, 9491(0F): 1–8.
- [4] M. M. Molenaar, D. Hill, P. Webster, E. Fidan, and B. Birch. "First downhole application of distributed acoustic sensing for hydraulic-fracturing monitoring and diagnostics," *SPE Drilling and Completion*, 2011, 7(2): 193–202.
- [5] A. Owen, G. Duckworth, and J. Worsley, "OptaSense: fiber optic distributed acoustic sensing for border monitoring," *Fiber Optic Sensors & Systems*, 2012, 26(8): 362–364.
- [6] J. C. Juarez, E. W. Maier, K. N. Choi, and H. F. Taylor, "Distributed fiber-optic intrusion sensor system," *Journal of Lightwave Technology*, 2005, 23(6): 2081–2087.
- [7] J. C. Juarez and H. F. Taylor, "Field test of a distributed fiber-optic intrusion sensor system for long perimeters," *Applied Optics*, 2007, 46(11): 1968–1971.
- [8] M. Zhang, S. Wang, Y. Zheng, Y. Yang, X. Sa, and L. Zhang, "Enhancement for  $\Phi$ -OTDR performance by using narrow linewidth light source and signal processing," *Photonic Sensors*, 2016, 6(1): 58–62.
- [9] F. Peng and X. Cao, "A hybrid  $\Phi$ /B-OTDR for simultaneous vibration and strain measurement," *Photonic Sensors*, 2016, 6(2): 121–126.
- [10] Y. Dong, L. Chen, and X. Bao, "Time-division multiplexing based BOTDA over 100 km sensing length," *Optics Letters*, 2011, 36(2): 277–279.
- [11] A. Minardo, A. Coscetta, R. Bernini, and L. Zeni, "Heterodyne slope-assisted Brillouin optical time-domain analysis for dynamic strain measurements," *Journal of Optics*, 2016, 18(2): 1–7.
- [12] X. Bao and L. Chen, "Recent progress in optical fiber sensors based on Brillouin scattering at University of Ottawa," *Photonic Sensors*, 2011, 1(2): 102–117.
- [13] Z. Sun, J. Wang, J. Chang, J. Ni, L. Min, C. Wang, *et al.*, "Fiber laser sensor interrogation system development and test," *SPIE*, 2012, 8351(1): 73–77.